μ-Lat: A High-Throughput Humanized Mouse Model to Evaluate Human Immunodeficiency Virus Eradication Strategies

Hannah S. Sperber[1,2,3*], Padma Priya Togarrati[1*], Kyle A. Raymond[1,3], Mohamed S. Bouzidi[1,3], Renata Gilfanova[1], Alan G. Gutierrez[1], Marcus O. Muench[1,3], and Satish K. Pillai[1,3+]

[1]Vitalant Research Institute, San Francisco, California, United States of America

[2]Free University of Berlin, Institute of Biochemistry, Berlin, Germany

[3]University of California, San Francisco, California, United States of America

*These authors contributed equally

+Corresponding author, e-mail: satish.pillai@ucsf.edu

Conflict of interest statement:

The authors have declared that no conflict of interest exists.

Abstract

A critical barrier to the development of a human immunodeficiency virus (HIV) cure is the lack of a scalable animal model that enables robust evaluation of eradication approaches prior to testing in humans. We established a humanized mouse model of latent HIV infection by transplanting "J-Lat" cells, Jurkat cells harboring a latent HIV provirus encoding an enhanced green fluorescent protein (GFP) reporter, into irradiated adult NOD.Cg-*Prkdc*^{scid} *Il2rg*^{tm1Wjl}/SzJ (NSG) mice. J-Lat cells exhibited successful engraftment in several tissues including spleen, bone barrow, peripheral blood, and lung, in line with the diverse natural tissue tropism of HIV. Administration of tumor necrosis factor (TNF)-α, an established HIV latency reversal agent, significantly induced GFP expression in engrafted cells across tissues, reflecting viral reactivation. These data suggest that the "**μ-Lat**" model enables efficient determination of how effectively viral eradication agents, including latency reversal agents, penetrate and function in diverse anatomical sites harboring HIV *in vivo*.

Keywords: Humanized mouse, HIV, HIV latency, latency reversal, shock and kill, antiviral gene therapy

Introduction

The advent of antiretroviral therapy (ART) has dramatically reduced morbidity and mortality for human immunodeficiency virus (HIV)-infected individuals with access to healthcare in resource-rich countries. However, despite years of potent therapy, eradication of infection is not achieved due to the persistence of HIV latently-infected cells during treatment(1). Accumulating evidence suggest that "non-AIDS" cardiovascular, renal and hepatic diseases are amplified by HIV infection, and the immune system may exhibit premature senescence even among patients with complete viral suppression(2). Moreover, although enormous progress has been made to provide ART in resource-limited settings, there are huge economic, political and operational challenges to reach the goal of universal access to lifelong treatment. These realities have created a pronounced interest in developing HIV cure strategies.

Elimination of the latent HIV reservoir is critical to achieving HIV eradication *in vivo*. A number of approaches are currently under investigation, including therapeutic vaccination, immunomodulatory approaches, ART intensification, therapeutic HIV latency reversal (the "shock and kill" strategy), as well as a number of gene therapy approaches(3,4). In all scenarios, it will be critical to have proper diagnostic tools and models in place to comprehensively evaluate performance and safety prior to deployment in a clinical setting. A critical barrier to the development of an HIV cure is the lack of an accessible and scalable preclinical animal model that enables robust evaluation of candidate eradication approaches prior to testing in humans(5). As a result, many promising curative approaches never graduate past the petri dish stage. Infection of nonhuman primates (NHP) with simian immunodeficiency virus (SIV) is an option and has been utilized extensively to study HIV/AIDS pathogenesis(6,7). Recent advancements have been made

in optimizing ART regimens to achieve durable virus suppression and thus enable evaluation of HIV cure strategies in the SIV-NHP model(8–10). However, biological limitations remain since this model uses SIV and might not recapitulate human host-HIV interactions and HIV latency mechanisms(11–15). In addition, NHP experiments involve complex ethical considerations, and the high costs and labor requirements only allow small numbers of animals to be utilized in any given trial, limiting statistical power and generalizability(11).

Mouse models represent another alternative with lower costs, more convenient husbandry requirements, as well as greater scalability. In the context of HIV studies, a wide range of small animal models have been developed comprising knockout mouse (16–18), transgenic mouse(19–23), and humanized mouse models(6,24–29). Humanized mice are established by xenotransplantation of human cells or tissues in immunodeficient mouse strains. Most strains used in HIV research are derivatives of severe combined immunodeficient (SCID) mice, which harbor mutations in the gene coding for a DNA-dependent protein kinase catalytic subunit (Prkdc). These mice are "humanized" using two approaches: 1) human cells are injected with or without prior irradiation of mice or 2) portions of tissue are surgically implanted. Different cells have been used for injection, including human peripheral blood mononuclear cells (PBMCs), as in the *hu-PBL-SCID* mouse model(30), obtained from healthy(31) or HIV-infected ART suppressed individuals(32), or human hematopoietic stem cells (HSCs), as in the *hu-HSC* mouse model(33), or the more recently developed *T-cell-only*(34) and *myeloid-only*(35) mouse models (*ToM* and *MoM*). Implantation of fetal thymus and liver tissue fragments are used for the *SCID-hu thy/liv*(36,37) and *bone marrow/liver/thymus* (BLT)(38,39) mouse models. Although all these model systems have contributed to our understanding of HIV pathogenesis and persistence, key

limitations remain that need to be addressed in order to fully exploit the potential of these small animal models in HIV cure research. *Hu-PBL-SCID* mice struggle with the development of graft versus host disease (GVHD) which renders this model inapplicable for long-term studies involving HIV persistence. The generation of *SCID-hu thy/liv* and BLT mice is limited due to the need for surgical implantation and a limited supply of tissue. Moreover, these models as well as *hu-HSC*, *ToM* and *MoM* mice rely on the engraftment of cells or tissues typically derived from human fetal specimens, which in light of recent changes in federal policies face significant challenges, as ethical, legal, and political considerations surrounding the use of fetal tissue in scientific research have made it increasingly difficult to obtain such material(40,41). A major limitation shared by all these models remains the low frequency of HIV latently-infected cells, which impacts the applicability of these models as robust *in vivo* test bases for HIV cure strategies.

In the present study, we therefore pursued a new approach and transplanted J-Lat 11.1 cells (J-Lat cells), which are Jurkat cells harboring a latent HIV provirus encoding an enhanced green fluorescent protein (GFP) reporter, into irradiated adult NOD.Cg-*Prkdc*^{scid} *Il2rg*^{tm1Wjl}/SzJ (NSG) mice. Our data show robust engraftment of J-Lat cells in several tissues three weeks after injection as well as significant reactivation of these latently-infected cells *in vivo* upon intravenous administration of the established latency reversal agent (LRA) tumor necrosis factor (TNF)-α. By applying an established and widely-utilized HIV latency reporter cell line(42–44), we circumvent the need for fetal or any other donor-derived tissue, and achieve high frequencies of HIV latently-infected cells *in vivo* on a short experimental time scale. In addition, the presence of the GFP reporter cassette in the integrated viral genome provides for quick and convenient assessment of viral reactivation using flow cytometry or microscopy. Moreover, by taking

advantage of the HIV reporter cell line, the "μ-Lat" humanized mouse model represents a highly reproducible platform that enables a simple transition from *in vitro* screening approaches to an *in vivo* system enabling the evaluation of bioavailability and pharmacokinetics of candidate regimens. Although not intended to serve as a pathophysiology model, we present this approach as a scalable, accessible, and cost-effective preclinical testbed to evaluate the safety, tolerability, and performance of HIV cure strategies in distinct anatomical niches.

Results

The human cell surface proteins CD147 and CD29 enable clear and reliable discrimination of J-Lat cells from mouse cells. Our model involves transplantation of J-Lat cells (immortalized human T cells harboring latent HIV provirus with a GFP reporter reflecting viral transcriptional activity) into irradiated adult NSG mice(42). We therefore searched for cell surface markers that reliably identify engrafted J-Lat cells in a background of mouse cells, exhibiting three key features: 1) universal expression across J-Lat cells, 2) high per-cell expression on J-Lat cells, and 3) absence of expression on the surface of mouse cells.

Our candidate panel included seven cell surface proteins commonly known to be expressed in human CD4+ T cells: CD45, CD4, TCR α/β, CD27, CD147, CD29, and HLA-ABC. Four of these cell surface proteins were found to be expressed universally among the J-Lat population: CD45, CD147, CD29 and HLA-ABC (**Figure 1A**). The mean fluorescence intensity (MFI) of the four proteins was measured, reflecting the relative abundance of each protein on the cell surface. CD147 exhibited the highest MFI, followed by CD29 (**Figure 1B**). We next tested if the CD29 and CD147 antibodies (both APC conjugated to achieve maximum signal to noise ratio in the APC-channel) showed detectable binding to mouse cells obtained from different tissues. We harvested bone marrow (BM), lung, brain, gut, intraepithelial lymphocytes (IEL) from gut tissue, lymph nodes, heart and spleen. In addition, based on Hoggatt et al.(45), who reported that blood parameters such as cell composition significantly varied depending on sampling manner and site, we performed peripheral blood (PB) harvest in three different ways: by retro-orbital bleed (r.-o.), tail vein bleed, or heart bleed. Human CD29 and CD147 staining was combined with antibodies targeting the mouse-specific lineage markers CD45, TER-119, and H-2K^d for a positive

identification of mouse cells. While 100% of cultured J-Lat cells expressed CD29 and CD147 and were negative for mouse-specific markers (**Figure 1C**), the frequency of $CD147^+/CD29^+$ cells was negligible or absent across mouse tissues (**Figure 1D and E**). Most tissues harbored 0% $CD147^+/CD29^+$ cells, while 0.06% $CD147^+/CD29^+$ cells were detected in the lung and 1.37% $CD147^+/CD29^+$ cells were detected in PB upon heart bleed (**Figure 1E**). For both samples, lung and PB heart bleed, these percentages represent a single event detected to be positive for CD147/CD29 (**Figure 1D and E**). Thus, we concluded that among the tested cell surface proteins, human CD147 combined with CD29 function as a reliable and specific marker pair for the identification of J-Lat cells engrafted in mouse tissues.

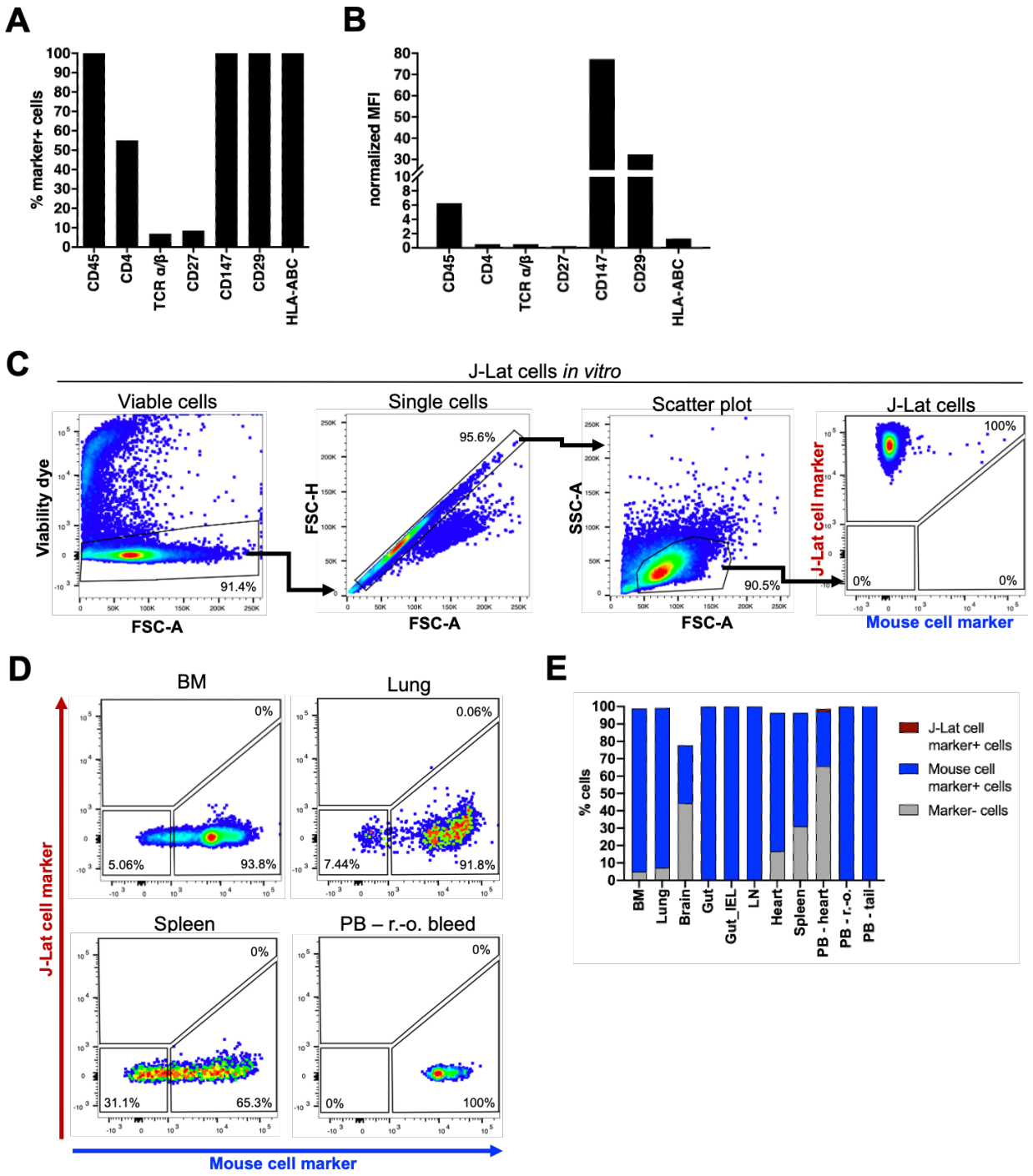

Figure 1: The cell surface proteins CD147 and CD29 are abundantly and specifically expressed in J-Lat 11.1 cells. 1 x 10^6 J-Lat cells were stained with antibodies targeting select cell surface proteins to (A) measure the frequency of marker-positive cells and (B) mean fluorescence intensity (MFI) of proteins on the cell surface using flow cytometry. The MFI of marker signal positive cells was normalized to signal positive cells of respective isotype control stained samples. A representative experiment is summarized in the bar graphs. (C) Gating strategy to identify human J-Lat cells upon multicolor staining with CD147/CD29-APC (J-Lat cell

marker) and CD45/TER-119/H-2Kd-Pacific Blue (mouse cell marker) *in vitro*. (D) Representative flow plots show multicolor staining of single cell suspensions prepared from different mouse tissues. Mouse cells were stained, measured, and analyzed in the same way as *in vitro* J-Lat cells to evaluate specificity and background signal of human CD29 and CD147 antibodies. Single cell suspensions were prepared from 8 mouse tissues and three different harvest methods for peripheral blood (PB) to determine the applicability of the multicolor staining for subsequent engraftment studies (E). BM = bone marrow, IEL = intraepithelial lymphocytes, LN = lymph node, PB = peripheral blood, r.-o. = retro-orbital.

Establishment and optimization of J-Lat cell engraftment in humanized mice. In the context of establishing a humanized mouse model, we examined and optimized several parameters simultaneously to achieve a highly reproducible and robust *in vivo* platform (**Figure 2**).

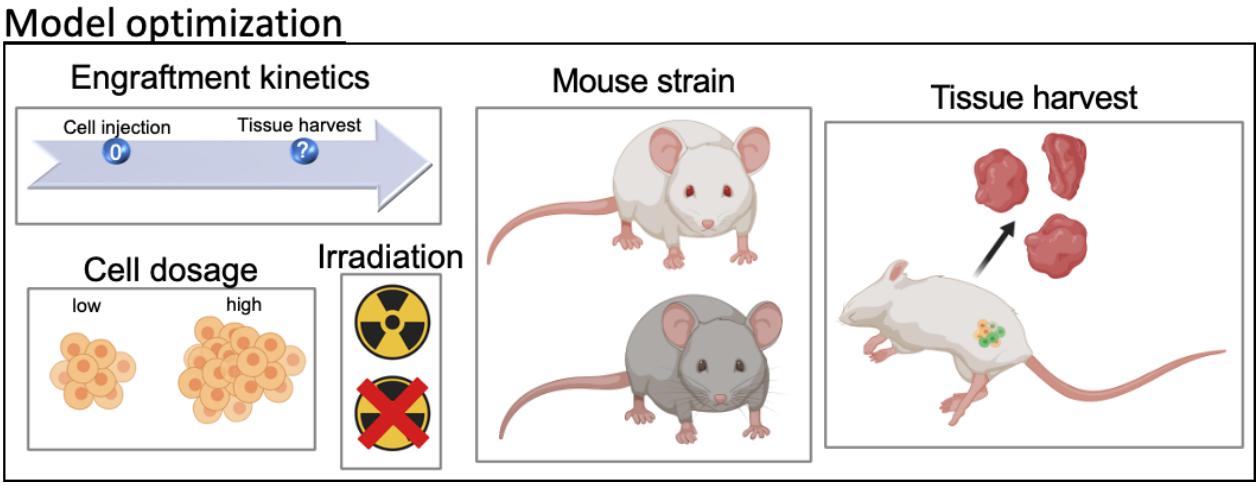

Figure 2: Schematic representation of parameters that were examined and optimized to establish the µ-Lat model. J-Lat cell engraftment kinetics, the J-Lat cell dosage, irradiation of recipient mice, and testing of J-Lat cell engraftment in different mouse strains is summarized in Figure 3. Evaluation of J-Lat cell engraftment levels in different mouse tissues is represented in **Figure 4**.

In the following pilot experiments, we focused on J-Lat cell engraftment in the BM (**Figure 3**). To measure the kinetics of J-Lat cell engraftment, we harvested the BM at different time points post J-Lat cell injection (**Figure 3A**). We examined the effect of varying cell doses (**Figure 3B**) and irradiation of recipient mice (**Figure 3C**) on J-Lat cell engraftment levels, and compared

engraftment levels in NOD.Cg-*Prkdc*^{scid} *Il2rg*^{tm1Wjl} Tg(CMV-IL3,CSF2,KITLG)1Eav/MloySzJ (NSG-3GS) and NSG mice (**Figure 3D**). J-Lat cell engraftment in the BM was detected 18 days post cell injection (pci) with 4.6±1.8% engrafted J-Lat cells, and reached significant levels 25 days pci compared to 1 and 3 days pci with an average of 16.3±8.6% engrafted J-Lat cells (**Figure 3A**). Using a J-Lat cell injection dose of 10 x 10^6 J-Lat cells compared to 5 x 10^6 J-Lat cells per mouse lead to higher but not significant engraftment levels with an average of 9.0±1.9% compared to 4.6±1.8% engrafted J-Lat cells in the BM of nonirradiated NSG-3GS mice (**Figure 3B**). Nonirradiated NSG-3GS recipient mice harbored 9.0±1.9% engrafted J-Lat cells in the BM compared to 12.3±1.4% engrafted J-Lat cells detected in irradiated NSG-3GS recipient mice (**Figure 3C**). Again, this difference was not significant but showed a slight increase in J-Lat cell engraftment levels when recipient mice were irradiated. Finally, when testing engraftment levels in different mouse strains, we found significantly higher J-Lat cell engraftment in NSG mice (**Figure 3D**). An average of 39.9±23.6% engrafted J-Lat cells was detected in the BM of NSG-3GS compared to 96.28±1.5% in the BM of NSG mice 3 week pci of 10 x 10^6 J-Lat cells (**Figure 3D**). Based on our results, we concluded that irradiation of recipient NSG mice and a cell dose of 10 x 10^6 J-Lat cells per mouse administered through intravenous injection resulted in efficient and reproducible cell engraftment levels which peaked 3 weeks following cell transplantation.

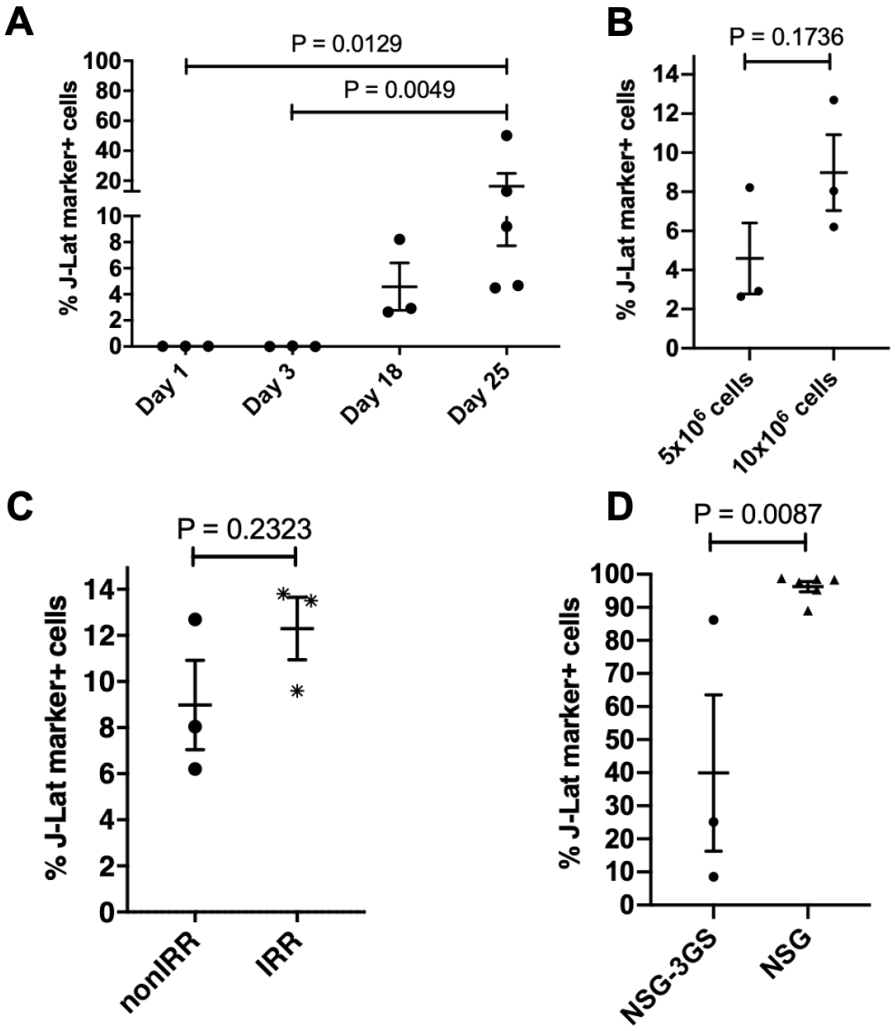

Figure 3: Optimal engraftment levels of J-Lat cells are achieved 3 weeks post injection in irradiated NSG mice using 10 x 10^6 J-Lat cells for transplantation. The parameters described in **Figure 2** were examined and optimized concomitantly by focusing on engraftment levels in the BM. (A) J-Lat cell engraftment kinetics: Nonirradiated NSG-3GS mice were transplanted with 5 x 10^6 J-Lat cells and the BM harvested at indicated time points post cell injection. (B) J-Lat cell injection dosage: J-Lat cell engraftment levels in the BM of nonirradiated NSG-3GS were compared using different initial injection cell doses of 5 x 10^6 J-Lat cells (BM harvested 18 days post cell injection) or 10 x 10^6 J-Lat cells (BM harvested 14 days post cell injection). (C) Irradiation of recipient mice: NSG-3GS recipient mice were nonirradiated (nonIRR) or irradiated (IRR) before transplantation of 10 x 10^6 J-Lat cells and engraftment levels determined two weeks post cell transplantation. (D) Mouse strain selection: 10 x 10^6 J-Lat cells were injected either into irradiated NSG-3GS or irradiated NSG mice and engraftment levels in the BM measured 3 weeks post cell injection and 24h post TNF-α treatment. Each dot represents an individual animal for the respective condition. Each plot represents an independent experiment with at least n ≤ 3. P values in (A) were determined using the nonparametric Kruskal-Wallis test with

the uncorrected Dunn's test for multiple comparisons. P values in (B-D) were determined using an unpaired, two-tailed t-test. A $P<0.05$ was considered as significant difference.

J-Lat cells engraft successfully in several tissues in transplanted NSG mice. Using the determined experimental conditions, we investigated J-Lat cell engraftment in a multitude of tissues, as listed above, that we harvested from 5 irradiated NSG mice 3 weeks pci (**Figure 4**). To analyze the expression of J-Lat and mouse markers on cells obtained from different mouse tissues, we followed the gating strategy as described before (see **Figure 1C and Figure 4A and B**). J-Lat cell engraftment levels were evaluated based on the frequency of $CD147^+/CD29^+$ cells, the MFI of $CD147^+/CD29^+$ cells, and the absolute number of $CD147^+/CD29^+$ cells in the respective processed tissues (**Figure 4C-E**). We found engrafted J-Lat cells in several tissues including the BM, brain, lung, spleen, and PB (**Figure 4A and B**). The mean frequency of engrafted J-Lat cells were 30.0±15.4% in the BM, 46.9±12.4% in the brain, 7.7±1.7% in the lung, and 0.7±0.4% in the spleen (**Figure 4C**). While the MFI of the engrafted J-Lat cells was comparable within and across these tissues, ranging from about 20,000 to 30,000 a.u. (**Figure 4D**), the absolute number of engrafted J-Lat cells varied drastically. We detected on average 3957.0±3563.0 J-Lat cells in the BM, 60.2±8.1 J-Lat cells in the lung and 37.0±25.1 J-Lat cells in the spleen, while the absolute number of engrafted J-Lat cells in the brain did not reach more than on average 5.8±2.3 cells (**Figure 4E**). When focusing on engraftment in the PB, we found that heart and r.-o. bleed yielded a substantial higher frequency of engrafted J-Lat cells with an average of 24.9±5.7% and 22.8±7.6% engrafted J-Lat cells compared to tail vein bleed with 0.7±0.4% engrafted J-Lat cells (**Figure 4C**). However, PB harvest by r.-o. bleeding showed the highest MFI and more important, the highest absolute number of engrafted J-Lat cells (mean heart = 6.2±1.2, mean r.-o. = 24.2±15.7, mean tail =

0.8±0.4) (**Figure 4D and E**). Thus, due to considerable engraftment levels and practicality of collection, we decided to harvest PB in subsequent experiments via r.-o. bleeding.

Based on these results, considering J-Lat cell frequency, MFI and absolute number of engrafted J-lat cells, we focused in subsequent experiments on J-Lat engraftment in the BM, lung, spleen and PB via r.-o. bleed and established a suitable engraftment and sample collection protocol to drive the model.

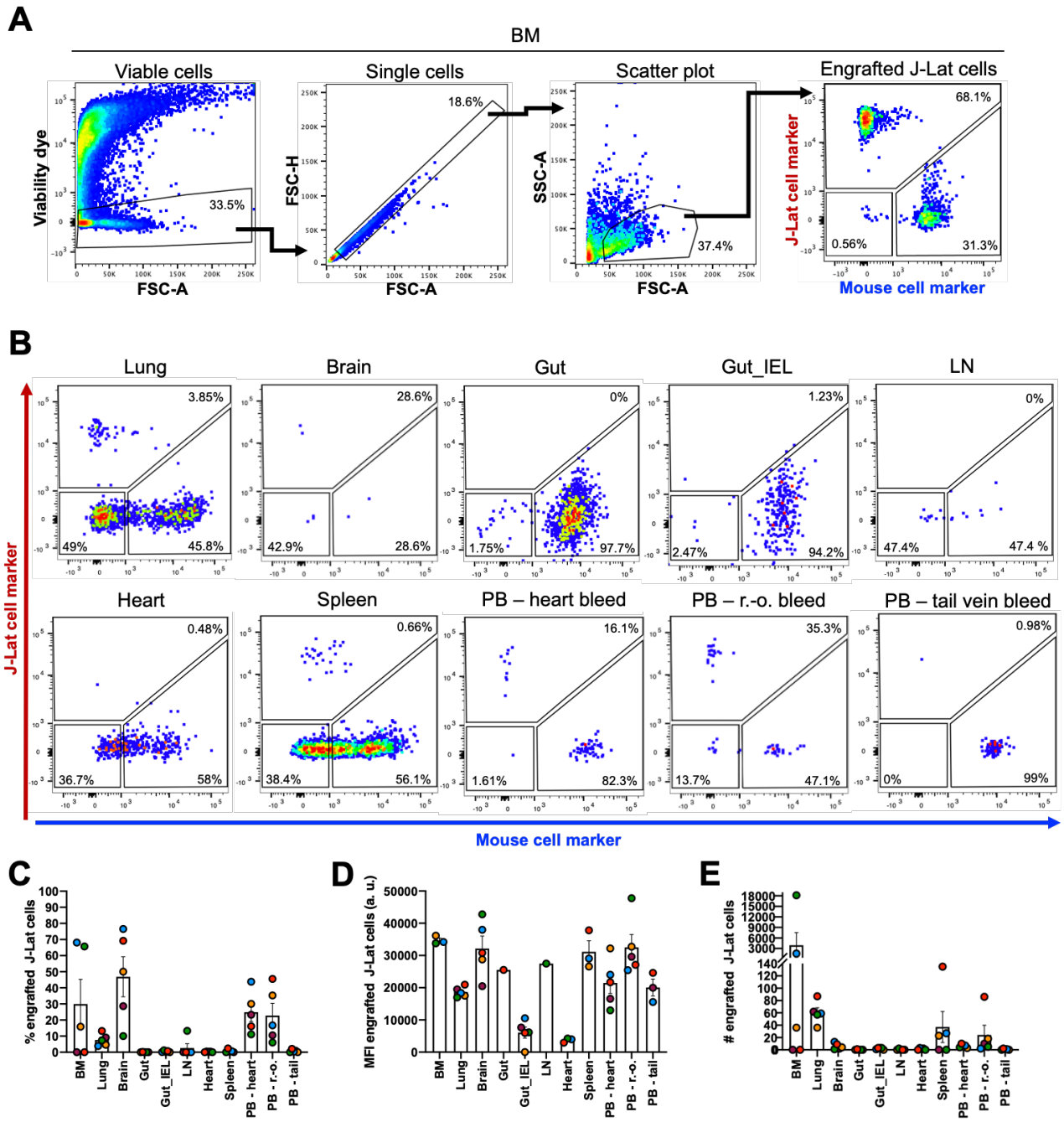

Figure 4: J-Lat cells engraft successfully in several tissues in transplanted NSG mice. (A) Gating strategy to identify human J-Lat cells in harvested mouse tissues as described before exemplified here with BM. (B) Representative flow plots are shown for engraftment levels across tissue sites observed at necropsy and engraftment levels in PB (n = 5) using three different harvest approaches: r.-o. bleeding, tail vein bleeding, and heart bleeding. (C-D) Bar graphs summarize engrafted J-Lat cell frequency (C), MFI of engrafted J-Lat cells (D), and number of engrafted J-Lat cells (E) in the respective tissue. Each data point represents an individual animal. Colors indicate tissues harvested from the same animal. Error bars show the standard error of the mean (SEM).

J-Lat cells maintain low GFP expression upon engraftment in selected tissues. Once we confirmed reproducible and robust engraftment in several tissues, we wanted to investigate GFP expression levels of engrafted J-Lat cells. As described before, the GFP reporter integrated into the latent provirus in J-Lat cells is under the control of the proviral LTR and thus reflects viral transcriptional activity. High GFP expression levels would thus indicate spontaneous viral reactivation *in vivo* and render the model inapplicable for testing LRAs. We measured J-Lat cell engraftment levels and GFP background signal of engrafted J-Lat cells in the selected tissues (BM, lung, spleen, PB r.-o.) of 10 NSG mice 3 weeks pci (**Figure 5**). We applied our previously described gating strategy to identify engrafted J-Lat cells based on CD147/CD29 expression and measured GFP signal within this compartment (**Figure 5A-C**). Engraftment of J-Lat cells was observed in the BM (mean = 37.9±13.3%), lung (mean = 5.7±0.6%), spleen (mean = 0.9±0.4%), and PB r.-o. (mean = 0.6±0.2%) (**Figure 5D**). Across these tissues, GFP expression levels of engrafted J-Lat cells remained at low levels with 4.0±1.2% GFP-positive cells in the BM, 2.1±0.3% GFP-positive cells in the lung, 2.0±0.9% GFP-positive cells in the spleen, and 2.2±1.1% GFP-positive cells in PB r.-o. (**Figure 5E**). The results showed that while these mouse tissues harbored substantial levels HIV latently-infected cells *in vivo,* engraftment of J-Lat cells in the tested tissues did not lead to spontaneous reactivation of viral transcription.

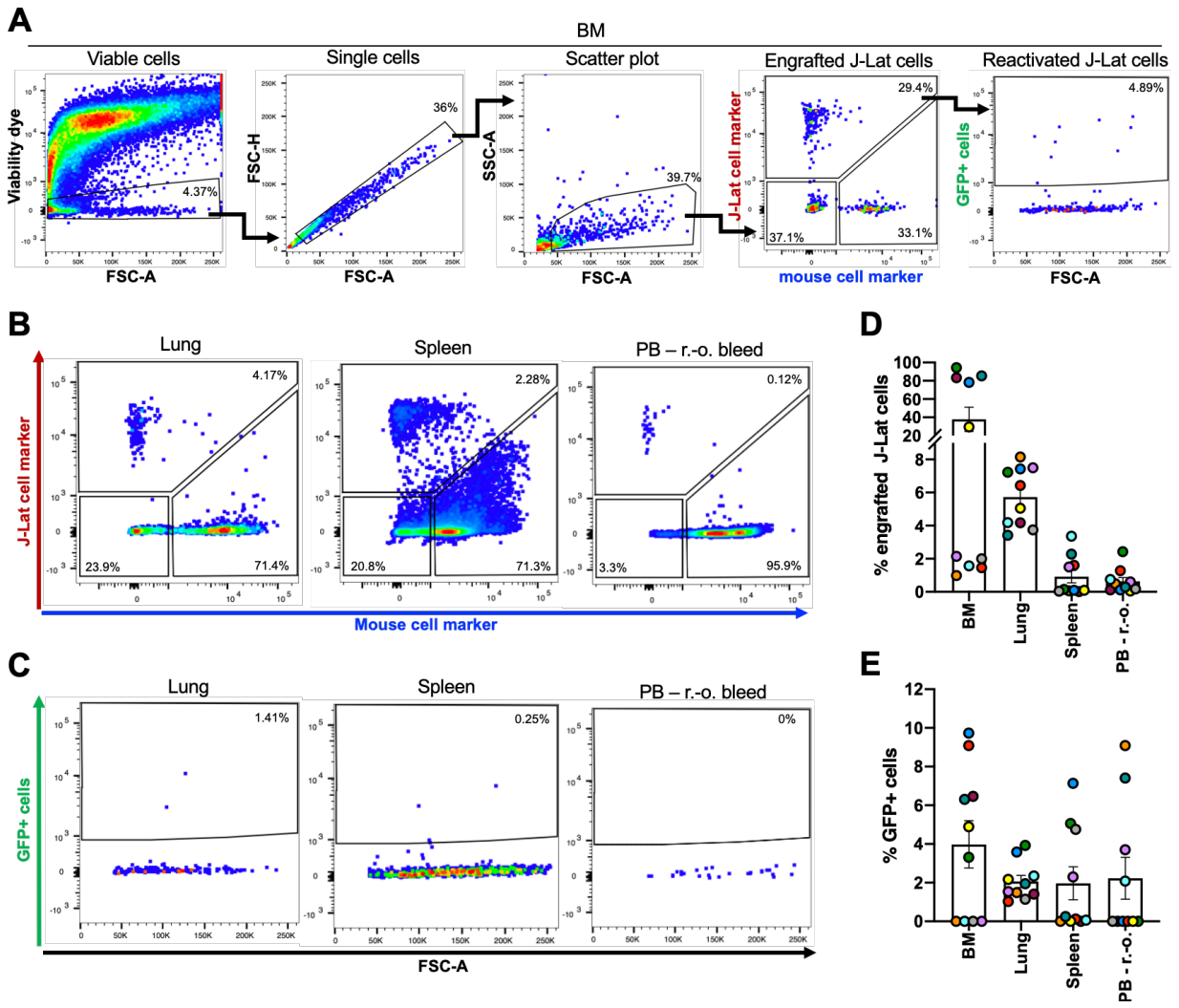

Figure 5: Engrafted J-Lat cells show low basal levels of GFP expression 3 weeks post cell transplantation. (A) Gating strategy to identify human J-Lat cells and GFP background signal of these in harvested mouse tissues illustrated here with a representative BM sample. Representative flow plots are shown for engraftment levels (B) and GFP background signal (C) across selected tissues observed at necropsy (n = 10). Bar graphs summarize engrafted J-Lat cell frequency (D) and GFP expression levels (E) of engrafted J-lat cells. Each data point represents an individual animal. Colors indicate tissues harvested from the same animal. Error bars show SEM.

TNF-α treatment induces GFP expression in tissue engrafted J-Lat cells reflecting reactivation of latent provirus *in vivo*. Finally, we sought to determine if HIV LRA administration would result

in viral reactivation *in vivo*. Viral reactivation was measured based on the frequency of GFP expressing cells within engrafted J-Lat cells following LRA treatment (**Figure 6A**).

The proviruses within the J-Lat family of clones were selected to be responsive to TNF-α stimulation, resulting in viral LTR-driven GFP expression(42). 24h *in vitro* treatment of J-Lat cells with 20 ng/µl TNF-α yielded an average of 30.7±7.4% GFP-positive cells compared to 61.0±3.8% GFP-positive cells upon 20 nM PMA / 1 µM Ionomycin treatment (positive control), whereas mock-treated (0.5% DMSO) and untreated cells were largely GFP-negative (mean = 1.2±0.3% and mean = 0.8±0.1%) (**Figure 6B**). Therefore, we performed *in vivo* reactivation experiments using 20 µg of TNF-α as an LRA (with PBS as a vehicle control)(46). 24h following TNF-α tail vein injection, effects on tissue engraftment and reactivation of latent provirus were estimated in a cross-sectional manner at necropsy, comparing 9 animals treated with TNF-α versus 10 vehicle control animals. Analyses of all tissues demonstrated no significant effect of TNF-α treatment on J-Lat cell engraftment levels within the respective compartment (**Figure 6C**), but revealed significant increases in the frequency of GFP-positive cells, reflecting viral reactivation (**Figure 6D**). Engrafted J-Lat cells obtained from mice treated with PBS as a vehicle control comprised 3.0±1.8% GFP-positive cells in the BM, 1.2±0.4% in spleen, 1.8±0.3% in the lung and 1.6±0.4% in PB (**Figure 6D**). Engrafted J-Lat cells obtained from TNF-α treated mice exhibited on average 9.7±4.0% GFP-positive cells in the BM, 21.4±3.6% in spleen, 21.1±2.0% in the lung, and 20.2±2.3% in PB (**Figure 6D**). Comparing the two populations (TNF-α vs vehicle control) demonstrated a GFP expression fold-change of 3.2 in the BM ($P = 0.0241$), 17.8 in the spleen ($P < 0.0001$), 11.7 in the lung ($P < 0.0001$) and 12.7 in the PB ($P < 0.0001$), illustrating potent and significant viral reactivation *in vivo*.

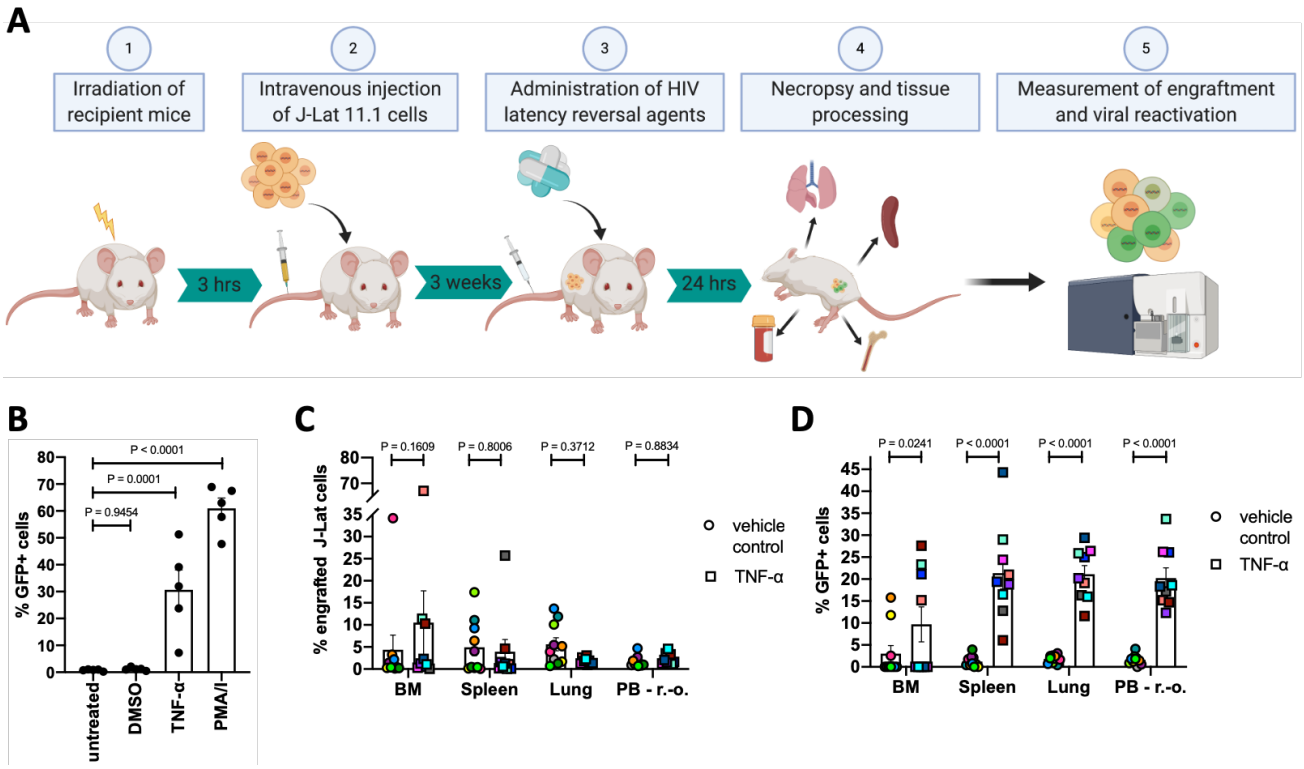

Figure 6: TNF-α treatment reactivates latent HIV *in vivo* in the µ-Lat model. (A) Schematic representation of the procedure to test LRAs *in vivo* using the µ-Lat model. (1) Mice receiving cells of interest for transplantation are irradiated 3 hours prior to cell injection. (2) Each mouse receives 10 x 10^6 J-Lat cells via intravenous injection. (3) Three weeks post injection (21 days) mice are treated for 24h with LRAs of interest, followed by (4) necropsy, tissue harvest and processing, and preparation of single-cell suspensions. (5) Single-cell suspensions are stained for J-Lat and mouse cell markers to assess engraftment levels via flow cytometry. Reactivation of latent provirus following LRA treatment is assessed by measuring GFP expression via flow cytometry (the J-Lat provirus contains an LTR-driven GFP reporter). (B) J-Lat cells were treated *in vitro* for 24h with 0.5% DMSO (vehicle control), 20 ng/µl TNF-α, 20 nM PMA/1 µM Ionomycin (positive control) or left untreated (negative control) to assess viral reactivation based on GFP expression (n = 5). (C) J-Lat engraftment levels were measured 24h post tail vein injection of 20 µg TNF-α (n = 9) or vehicle control (PBS, n = 10) in BM, spleen, lung and PB of mice. (D) Effect of TNF-α on viral reactivation (GFP expression), comparing animals treated with TNF-α versus vehicle control. One-way ANOVA and uncorrected Fisher's LSD for multiple comparisons was used to analyze *in vitro* reactivation data (B) and mixed effects model and uncorrected Fisher's LSD for multiple comparisons was used for *in vivo* engraftment (C) and reactivation data (D). Colors indicate specific animals and tissues obtained from the same animal. Error bars show SEM.

Discussion

The development of an HIV cure will be accelerated by the deployment of a convenient and cost-effective animal model that enables the determination of an agent's therapeutic efficacy as it navigates through tissue-specific barriers and the circulatory, respiratory and excretory systems. We present a novel humanized mouse model of HIV latency that aims to address this gap. In this study, we established a reliable method to discriminate between J-Lat and mouse cells (**Figure 1** and **Figure 4**) and demonstrated robust engraftment of these cells in multiple tissues sites (**Figure 4** and **Figure 5**). Significant viral reactivation was observed in TNF-α-treated animals with respect to vehicle control-treated animals (**Figure 6D**). Importantly, although *in vivo* treatment with TNF-α induced GFP expression and thus viral reactivation by 3.2 (BM), 17.8 (spleen), 11.7 (lung), and 12.7 (PB) -fold compared to vehicle control treated animals (**Figure 6D**), TNF-α treatment *in vitro* induced a 25.3-fold increase in GFP expressing cells (**Figure 6B**), emphasizing the importance of testing promising and potent regimens and their efficacy beyond *in vitro* cultures in an *in vivo* system.

Although not intended to serve as a pathophysiology model, the μ-Lat platform offers key advantages over existing preclinical models focused on HIV eradication. Firstly, the model is highly efficient; the timeframe to generate mouse colonies that are ready for administration of experimental therapies is approximately three weeks. In comparison, even the simplified humanized mouse model introduced by Kim et al.(31) requires four weeks for robust engraftment of intraperitoneally injected human PBMCs in NSG mice and an additional 5 weeks of incubation upon HIV infection. Secondly, the presence of the GFP reporter cassette in the integrated J-Lat viral genome allows for rapid and convenient assessment of HIV latency reversal

in vivo, eliminating the requirement for PCR or culture-based diagnostics to determine LRA potency. Thirdly, the model is characterized by high frequencies of HIV latently-infected cells (e.g. in some experiments exceeding 30% engraftment in BM), and these cells are distributed in a number of relevant anatomical sites that are central to HIV persistence. This stands in contrast to organoid-based models (e.g. the *SCID-hu thy/liv* mouse model) that exclusively involves viral colonization within a xenografted tissue(47). Lastly, the model is highly scalable due to the low costs and limited labor requirements of the method involving the easily and widely available J-Lat cell line (provided free of charge via the NIH AIDS Reagent Program). Importantly, the clonal nature of cell lines promotes consistency and high reproducibility across laboratories, while allowing for an easy transition from the petri-dish stage to an *in vivo* evaluation system.

Similar to any other animal model system, there are certain caveats associated with the μ-Lat model that should be considered. The efficiency of the model is largely driven by the administration of an HIV latently-infected cell line, rather than differentiated primary cells. As presented here, a single latent clone with a single proviral integration site was injected into mice. Proviral integration site is known to affect viral latency and responsiveness to LRA administration(48–50). However, this issue could be ameliorated by mixing different HIV latently-infected cell clones at specific ratios, thereby achieving higher integration site heterogeneity to more accurately represent *in vivo* variability. For instance, there are 11 J-Lat clones currently available via the NIH AIDS Reagent Program, each of which is characterized by a distinct proviral integration site. These clones often behave differently from each other as well when exposed to LRAs *in vitro*, likely reflecting a diversity of molecular mechanisms reinforcing viral latency across

clones(43). This mechanistic diversity could further enhance the predictive potential of the μ-Lat model.

Beyond concerns regarding integration site heterogeneity, the immortalized nature of the J-Lat cell line may impact molecular and regulatory pathways that affect HIV latency. However, the widespread usage of the J-Lat model and its derivative clones to examine viral latency and to evaluate the efficacy of HIV cure strategies *in vitro* speak to the model's utility(51–60). Ample data from primary cell-based models of latency and experiments involving *ex vivo* administration of LRAs to cells obtained from HIV-infected individuals on ART suggest that differences between applied models and between individuals can have dramatic effects on the establishment, maintenance, and reversal of HIV latency(43,61,62). Moreover, profiling of HIV latency in multiple tissue sites has demonstrated that the nature of viral latency may even vary extensively within a single infected individual(63–65). Therefore, it needs to be considered that any applied model system or cells from any given individual will influence predicted responses for the general population with a certain bias, just as a cell line-based system(26).

Our work described here represents a proof of concept, demonstrating that the engraftment of a cell line-based model of HIV latency may constitute a useful testbed for HIV cure strategies. This general approach is highly versatile and should allow for a broad range of infected cell types to be examined *in vivo*. For example, HIV latency in the myeloid compartment is likely critical to viral persistence(35,66–69), and multiple reports suggest this compartment may respond quite differently to curative approaches, as compared to lymphoid reservoirs(70,71). It may be fruitful to inject the U1 HIV chronically-infected promonocytic cell line(72) into NSG mice to examine LRA responses in myeloid cells. Building further on the myeloid theme, the central nervous system

(CNS) compartment is an important viral sanctuary site in the setting of ART(71,73–76), and HIV eradication approaches will almost certainly face unique challenges in this niche(76,77). As direct injection of human cells into the murine CNS has been used successfully as an engraftment approach(78–82), site-specific injection of the recently developed HC69.5 HIV latently-infected microglial cell line(83,84) into the brains of NSG mice may provide a convenient platform to gauge CNS-focused cure strategies.

Beyond preclinical investigation of LRAs, the μ-Lat framework may provide a convenient model system to evaluate gene therapy-based HIV eradication approaches. Gene therapy approaches targeting HIV infection generally fall into two categories: 1) Gene editing can be used to target or "excise" the HIV provirus directly in infected cells as an eradication approach(85,86) or 2) Editing can be used to modulate host cells to render them refractory to HIV infection and/or potentiate antiviral immune responses(87). In the former case, *in vivo* delivery of the gene therapy modality will likely be necessary to pervasively attack the HIV reservoir within a broad range of tissue sites in infected individuals. The μ-Lat model is well-suited to investigate gene delivery in this context, as it is characterized by robust engraftment of HIV latently-infected cells into diverse anatomical niches. This will allow for efficient assessment of gene therapy vector dissemination and antiviral function across anatomic sites. The LTR-driven GFP cassette within the J-Lat integrated provirus may facilitate this assessment; direct targeting of the GFP sequence may be used to examine vector trafficking and delivery, while specific targeting of the HIV LTR as a cure approach would be associated with a convenient readout (relative loss of GFP expression upon induced latency reversal).

In summary, the μ-Lat model is optimized for efficient and scalable evaluation of select HIV eradication approaches *in vivo*, allowing determination of therapeutic efficacy in addition to essential safety, tolerability, and pharmacokinetic parameters. Further development and diversification of the μ-Lat model system may enable convenient testing of HIV eradication approaches, including antiviral gene therapy strategies, in a range of cell types and tissue sites *in vivo*.

Materials and Methods

Cell culture and treatment: J-Lat 11.1 cells (kindly provided by Dr. Eric Verdin's lab) contain integrated latent full-length HIV genome harboring a mutation in the *env* gene and GFP in place of the *nef* gene as reporter for transcriptional activity of the provirus(88). J-Lat 11.1 cells were grown in media composed of RPMI 1640 (Gibco) supplemented with 10% fetal bovine serum (FBS) (Corning) and 1% Penicillin-Streptomycin (Gibco). Cells were cultured at 37°C in a humidified incubator containing 5% CO_2. To test potency of latency reversal agents (LRAs), 1 x 10^6 cells in 1 ml RPMI were left untreated (negative control), incubated in 0.5% DMSO (vehicle control), 20 nM PMA/1 µM Ionomycin (positive control) or 20 ng/µl TNF-α for 24h.

Mice: The work was approved by the Institutional Animal Care and Use Committee guidelines at Covance Laboratories, Inc. (San Carlos, CA) under Animal Welfare Assurance A3367-01 and protocol number IAC 2185 / ANS 2469. Animal husbandry was carried out according to the recommendations in the Guide for the Care and Use of Laboratory Animals of the National Institutes of Health. Mice were sacrificed in accordance with the guidelines from the American Veterinary Medical Association.

Adult female and male mice (≥8 weeks old) were included in this study and were maintained at the Vitalant Research Institute (VRI). Breeding pairs of NSG mice were obtained from Jackson Laboratories (Bar Harbor, ME), and were bred and maintained at VRI in a vivarium free from >40 murine pathogens as determined through biannual nucleic acid testing (Mouse Surveillance Plus PRIA; Charles River) of sentinel mice exposed to mixed bedding. Mice were maintained in sterile, disposable microisolator cages (Innovive, Inc.), which were changed every 14 days.

Environmental enrichment was provided by autoclaved cotton Nestlets (Ancare Corp.) and GLP-certified Bio-Huts (Bio-Serv). Feed consisted of sterile, irradiated diet of Teklad Global 19% protein diet (Envigo) with free access to sterile-filtered, acidified water (Innovive, Inc.). Several days prior to radiation and 3 weeks following radiation, mice were fed with irradiated Global 2018 rodent diet with 4100 ppm Uniprim® (Envigo).

J-Lat cell surface marker staining: For each staining, 1 x 10^6 J-Lat cells were washed once with PBS (Gibco), resuspended in 100 µl PBS, and stained with Zombie dye (Cat. #423105, BioLegend) according to manufacturer's protocol (1:100 dilution) to enable subsequent discrimination between live and dead cells. 10 min after incubation with the Zombie dye, human CD45-PE (clone HI30, Cat. #304039, BioLegend), CD4-PE (clone OKT4, Cat. #317410, BioLegend), TCR α/β-PE (clone IP26, Cat. #306708, BioLegend), CD27-PE (clone M-T271, Cat. #356406, BioLegend), CD147-APC (clone HIM6, Cat. #306214, BioLegend), CD29-APC (clone TS2/16, Cat. #303008, BioLegend), and HLA-ABC-APC/Cy7 (clone W6/32, Cat. #311426, BioLegend) antibodies were added respectively, and were incubated for another 20-30 min at room temperature (RT) in the dark. Cells were then washed with 2 ml of cell staining buffer (Cat. #420201, BioLegend), resuspended in 300 µl PBS and measured using an LSR II flow cytometer (BD Biosciences). Respective Isotype stained samples were used as control. At least 10,000 events were recorded for each sample.

J-Lat cell transplantation into mice: If not otherwise stated, J-Lat cell transplantation was performed as follows: mice were irradiated with 175 cGy radiation dose using a RS2000 X-Ray Biological Irradiator (RAD Source Technologies, Inc.) 3 hours prior to cell transplantation. Mice were transplanted with 10 x 10^6 J-Lat cells in a volume of 200 µl by tail vein injection. J-Lat cell

transplanted mice as well as control mice (left untransplanted) were sacrificed and analyzed within 25 days of cell transplantation.

Engraftment analysis of J-Lat cells in mice by flow cytometry: Transplanted mice were sacrificed by cervical dislocation 3 weeks post injection (or as indicated in figure legends). In one experiment, BM, brain, gut, intraepithelial lymphocytes (IEL) from gut tissue, heart, spleen, lung, lymph nodes, and PB were harvested. In subsequent experiments, selected tissues were harvested including BM, spleen, lung, and PB. Single cell suspensions from the BM, spleen, and PB were prepared as described previously by Beyer et al.(89). Brain, gut, heart, lymph node, and lung specimens were processed as follows: after harvest, all samples were stored in PBS on ice. Brain and lymph node specimens were washed twice in PBS, brain specimens additionally cut into small fragments (3-4 mm^2), followed by mashing the tissue fragments with a pestle and passaging the cell suspensions through 70 µm cell strainers. Gut, heart, and lung specimens were washed twice with PBS and then cut into 3-4 mm^2 pieces in a petri dish in 1 ml digestion solution consisting of 1 mg/ml DE Collagenase (Cat. #011-1040, VitaCyte) and 100 U/ml DNase I (Cat. #D5025-15KU, Sigma-Aldrich) final concentration in HBSS (Gibco). Fragments were transferred to 50 ml falcon tubes, digestion solution was added to a final volume of up to 5 ml, and samples were incubated at 37°C for 30 min (gut, heart) or 50 min (lung). IEL from gut tissue were isolated as supernatant after digestion incubation. Afterwards, up to 5 ml of stop solution, consisting of 0.5% BSA (Cat. #A2153, MilliPoreSigma) and 2 mM EDTA (Cat. #E0306, Teknova) final concentration in PBS, was added to each sample to end the enzymatic digestion reaction. Single cell suspensions were prepared by passage through a 70 µm cell strainer and washed with PBS. For the analysis of J-Lat cell engraftment, single cells from harvested mouse tissues were stained

with human CD147-APC or human CD147-APC combined with human CD29-APC, and additional Pacific Blue conjugate, mouse-specific lineage markers including CD45-Pacific Blue (clone 30-F11, Cat. #103126, BioLegend), TER-119-Pacific Blue (clone TER-119, Cat. #116232, BioLegend), and H-2K^{D}-Pacific Blue antibodies (clone SF1-1.1, Cat. #116616, BioLegend). Cells were incubated for 30 min at RT in the dark. Zombie dye staining detected in the APC-Cy7 channel was used for discrimination of live and dead cells. Following staining, cells were washed and run on an LSR II flow cytometer, where at least 10,000 events were recorded per sample. Flow cytometry data were analyzed using FlowJo software (FlowJo, Inc.).

Treatment of J-Lat engrafted mice with latency reversal agent TNF-α: Mice engrafted with J-Lat cells were treated with recombinant human TNF-α (Cat. #PHC3011, Gibco), a potent and well-known LRA. Briefly, NSG mice were transplanted with J-Lat cells and 3 weeks post-transplantation, mice received TNF-α (diluted in 200 µl PBS) intravenously at a dose of 20 µg/mouse(46). NSG mice injected with J-Lat cells and treated with PBS were used as vehicle control group.

After 24h of TNF-α treatment, mice were sacrificed to determine viral reactivation in PB, BM, lung and spleen tissues. Latency reversal of the HIV provirus was analyzed by comparing GFP expression of J-Lat cells in tissues of TNF-α treated mice vs the vehicle control group. GFP expression of engrafted J-Lat cells was determined by flow cytometry as described above.

Data analysis: All data were analyzed using GraphPad Prism version 8.2 and are presented as mean ± the standard error of the mean (SEM). Applied statistical tests and analyses are described

in figure legends. A P value of ≤0.05 was considered as statistically significant. Individual P values are indicated in figures.

Author contributions

HSS, PPT, KAR, MSB conceived and performed experiments; PPT, RG, AGG, MOM performed *in vivo* experiments; HSS, PPT collected and analyzed the data; HSS, PPT, MOM, SKP designed the study and wrote the manuscript.

Acknowledgments

This study was supported by the National Institutes of Health grants R01 AI150449 (SKP) and (SKP), and was additionally supported by a grant from the National Institutes of Health, University of California San Francisco-Gladstone Institute of Virology & Immunology Center for AIDS Research (P30 AI027763). We thank Dr. Roland Schwarzer for valuable input and careful review of the manuscript.

References

1. Wong JK, Hezareh M, Günthard HF, Havlir D V, Ignacio CC, Spina CA, et al. Recovery of replication-competent HIV despite prolonged suppression of plasma viremia. Science (80-) [Internet]. 1997 Nov 14 [cited 2019 Nov 15];278(5341):1291–5. Available from: http://www.ncbi.nlm.nih.gov/pubmed/9360926

2. Piot P, Bartos M, Ghys PD, Walker N, Schwartländer B. The global impact of HIV/AIDS. Nature [Internet]. 2001 Apr 19 [cited 2019 Nov 15];410(6831):968–73. Available from: http://www.nature.com/articles/35073639

3. Pitman MC, Lau JSY, McMahon JH, Lewin SR. Barriers and strategies to achieve a cure for HIV. Lancet HIV [Internet]. 2018 Jun [cited 2019 Nov 15];5(6):e317–28. Available from: https://linkinghub.elsevier.com/retrieve/pii/S2352301818300390

4. Schwarzer, Gramatica, Greene. Reduce and Control: A Combinatorial Strategy for Achieving Sustained HIV Remissions in the Absence of Antiretroviral Therapy. Viruses [Internet]. 2020 Feb 8;12(2):188. Available from: https://www.mdpi.com/1999-4915/12/2/188

5. Policicchio BB, Pandrea I, Apetrei C. Animal Models for HIV Cure Research. Front Immunol [Internet]. 2016 Jan 28 [cited 2019 Nov 15];7(JAN):12. Available from: http://www.ncbi.nlm.nih.gov/pubmed/26858716

6. Nixon CC, Mavigner M, Silvestri G, Garcia JV. In vivo models of human immunodeficiency virus persistence and cure strategies. J Infect Dis. 2017;215(Suppl 3):S142–51.

7. Denton PW, Søgaard OS, Tolstrup M. Using animal models to overcome temporal, spatial and combinatorial challenges in HIV persistence research. J Transl Med [Internet]. 2016 Dec 9;14(1):44. Available from: http://www.translational-medicine.com/content/14/1/44

8. Shytaj IL, Norelli S, Chirullo B, Della Corte A, Collins M, Yalley-Ogunro J, et al. A highly intensified ART regimen induces long-term viral suppression and restriction of the viral reservoir in a simian AIDS model. PLoS Pathog. 2012;8(6).

9. Dinoso JB, Rabi SA, Blankson JN, Gama L, Mankowski JL, Siliciano RF, et al. A Simian Immunodeficiency Virus-Infected Macaque Model To Study Viral Reservoirs That Persist during Highly Active Antiretroviral Therapy. J Virol. 2009;83(18):9247–57.

10. North TW, Higgins J, Deere JD, Hayes TL, Villalobos A, Adamson L, et al. Viral Sanctuaries during Highly Active Antiretroviral Therapy in a Nonhuman Primate Model for AIDS. J Virol. 2010;84(6):2913–22.

11. Kumar N, Chahroudi A, Silvestri G. Animal models to achieve an HIV cure. Curr Opin HIV AIDS [Internet]. 2016 Jul;11(4):432–41. Available from: https://linkinghub.elsevier.com/retrieve/pii/S0031938416312148

12. Sayah DM, Sokolskaja E, Berthoux L, Luban J. Cyclophilin A retrotransposition into TRIM5 explains owl monkey resistance to HIV-1. Nature [Internet]. 2004 Jul 7;430(6999):569–73. Available from: http://www.nature.com/articles/nature02777

13. Mariani R, Chen D, Schröfelbauer B, Navarro F, König R, Bollman B, et al. Species-specific exclusion of APOBEC3G from HIV-1 virions by Vif. Cell. 2003;114(1):21–31.

14. Baldauf HM, Pan X, Erikson E, Schmidt S, Daddacha W, Burggraf M, et al. SAMHD1 restricts HIV-1 infection in resting CD4 + T cells. Nat Med. 2012;18(11):1682–7.

15. Manel N, Littman DR. Hiding in plain sight: How HIV evades innate immune responses. Cell [Internet]. 2011;147(2):271–4. Available from: http://dx.doi.org/10.1016/j.cell.2011.09.010

16. Rehwinkel J, Maelfait J, Bridgeman A, Rigby R, Hayward B, Liberatore RA, et al. SAMHD1-dependent retroviral control and escape in mice. EMBO J [Internet]. 2013;32(18):2454–62. Available from: http://dx.doi.org/10.1038/emboj.2013.163

17. Behrendt R, Schumann T, Gerbaulet A, Nguyen LA, Schubert N, Alexopoulou D, et al. Mouse SAMHD1 Has Antiretroviral Activity and Suppresses a Spontaneous Cell-Intrinsic Antiviral Response. Cell Rep [Internet]. 2013 Aug;4(4):689–96. Available from: https://linkinghub.elsevier.com/retrieve/pii/S2211124713003999

18. Wittmann S, Behrendt R, Eissmann K, Volkmann B, Thomas D, Ebert T, et al. Phosphorylation of murine SAMHD1 regulates its antiretroviral activity. Retrovirology. 2015;12(1):1–15.

19. Seay K, Qi X, Zheng JH, Zhang C, Chen K, Dutta M, et al. Mice Transgenic for CD4-Specific Human CD4, CCR5 and Cyclin T1 Expression: A New Model for Investigating HIV-1 Transmission and Treatment Efficacy. PLoS One. 2013;8(5).

20. Rahim MMA, Chrobak P, Hu C, Hanna Z, Jolicoeur P. Adult AIDS-Like Disease in a Novel Inducible Human Immunodeficiency Virus Type 1 Nef Transgenic Mouse Model: CD4+ T-

Cell Activation Is Nef Dependent and Can Occur in the Absence of Lymphophenia. Vol. 83, Journal of Virology. 2009. p. 11830–46.

21. Hanna Z, Weng X, Kay DG, Poudrier J, Lowell C, Jolicoeur P. The Pathogenicity of Human Immunodeficiency Virus (HIV) Type 1 Nef in CD4C/HIV Transgenic Mice Is Abolished by Mutation of Its SH3-Binding Domain, and Disease Development Is Delayed in the Absence of Hck. Vol. 75, Journal of Virology. 2001. p. 9378–92.

22. Dickie P, Felser J, Eckhaus M, Bryant J, Silver J, Marinos N, et al. HIV-associated nephropathy in transgenic mice expressing HIV-1 genes. Virology. 1991;185(1):109–19.

23. Maung R, Hoefer MM, Sanchez AB, Sejbuk NE, Medders KE, Desai MK, et al. CCR5 Knockout Prevents Neuronal Injury and Behavioral Impairment Induced in a Transgenic Mouse Model by a CXCR4-Using HIV-1 Glycoprotein 120. J Immunol [Internet]. 2014 Aug 15;193(4):1895–910. Available from: https://linkinghub.elsevier.com/retrieve/pii/S0031938416312148

24. Marsden MD, Zack JA. Studies of retroviral infection in humanized mice. Virology [Internet]. 2015 May;479–480(1):297–309. Available from: https://linkinghub.elsevier.com/retrieve/pii/S004268221500029X

25. Victor Garcia J. Humanized mice for HIV and AIDS research. Curr Opin Virol. 2016;19:56–64.

26. Whitney JB, Brad Jones R. In Vitro and In Vivo Models of HIV Latency. In: Zhang L, Lewin SR, editors. HIV Vaccines and Cure : The Path Towards Finding an Effective Cure and

Vaccine [Internet]. Singapore: Springer Singapore; 2018. p. 241–63. Available from: https://doi.org/10.1007/978-981-13-0484-2_10

27. Krishnakumar V, Durairajan SSK, Alagarasu K, Li M, Dash AP. Recent updates on mouse models for human immunodeficiency, influenza, and dengue viral infections. Viruses. 2019;11(3).

28. Zhou J, Takahashi M, Burnett JC, Li S, Rossi JJ, Li H, et al. HIV Replication and Latency in a Humanized NSG Mouse Model during Suppressive Oral Combinational Antiretroviral Therapy. J Virol. 2018;92(7):e02118-17.

29. Lai F, Chen Q. Humanized mouse models for the study of infection and pathogenesis of human viruses. Vol. 10, Viruses. 2018. p. 1–17.

30. Mosier DE, Gulizia RJ, Baird SM, Wilson DB. Transfer of a functional human immune system to mice with severe combined immunodeficiency. Nature. 1988;335(6187):256–9.

31. Kim KCKC, Choi BS, Kim KCKC, Park KH, Lee HJ, Cho YK, et al. A Simple Mouse Model for the Study of Human Immunodeficiency Virus. AIDS Res Hum Retroviruses. 2016;32(2):194–202.

32. Flerin NC, Bardhi A, Zheng JH, Korom M, Folkvord J, Kovacs C, et al. Establishment of a Novel Humanized Mouse Model To Investigate In Vivo Activation and Depletion of Patient-Derived HIV Latent Reservoirs. Silvestri G, editor. J Virol [Internet]. 2019 Jan 9;93(6):1–18. Available from: http://jvi.asm.org/lookup/doi/10.1128/JVI.02051-18

33. Lapidot T, Pflumio F, Doedens M, Murdoch B, Williams DE, Dick JE. Cytokine stimulation of

multilineage hematopoiesis from immature human cells engrafted in SCID mice. Science (80-) [Internet]. 1992;255(5048):1137–41. Available from: https://science.sciencemag.org/content/255/5048/1137

34. Honeycutt JB, Wahl A, Archin N, Choudhary S, Margolis D, Garcia J V. HIV-1 infection, response to treatment and establishment of viral latency in a novel humanized T cell-only mouse (TOM) model. Retrovirology [Internet]. 2013;10(1):1. Available from: Retrovirology

35. Honeycutt JB, Wahl A, Baker C, Spagnuolo RA, Foster J, Zakharova O, et al. Macrophages sustain HIV replication in vivo independently of T cells Find the latest version : Macrophages sustain HIV replication in vivo independently of T cells. J Clin Invest. 2016;126(4):1353–66.

36. McCune J, Namikawa R, Kaneshima H, Shultz L, Lieberman M, Weissman I. The SCID-hu mouse: murine model for the analysis of human hematolymphoid differentiation and function. Science (80-) [Internet]. 1988 Sep 23;241(4873):1632–9. Available from: https://science.sciencemag.org/content/241/4873/1632

37. Namikawa R, Weilbaecher KN, Kaneshima H, Yee EJ, McCune JM. Longterm human hematopoiesis in the SCID-hu mouse. J Exp Med. 1990;172(4):1055–63.

38. Lan P, Tonomura N, Shimizu A, Wang S, Yang YG. Reconstitution of a functional human immune system in immunodeficient mice through combined human fetal thymus/liver and CD34+ cell transplantation. Blood. 2006;108(2):487–92.

39. Melkus MW, Estes JD, Padgett-Thomas A, Gatlin J, Denton PW, Othieno FA, et al.

Humanized mice mount specific adaptive and innate immune responses to EBV and TSST-1. Nat Med. 2006;12(11):1316–22.

40. Furgatch N. UCSF HIV/AIDS research intersects with abortion debate amid federal regulations. The Daily Californian [Internet]. 2019 Jun; Available from: https://www.dailycal.org/2019/06/26/ucsf-hiv-aids-research-intersects-with-abortion-debate-amid-federal-regulations/

41. McCune JM, Weissman IL. The Ban on US Government Funding Research Using Human Fetal Tissues: How Does This Fit with the NIH Mission to Advance Medical Science for the Benefit of the Citizenry? [Internet]. Vol. 13, Stem Cell Reports. 2019 [cited 2019 Nov 19]. p. 777–86. Available from: http://www.ncbi.nlm.nih.gov/pubmed/31722191

42. Jordan A, Bisgrove D, Verdin E. HIV reproducibly establishes a latent infection after acute infection of T cells in vitro. 2003 [cited 2017 Jun 26];22(8). Available from: https://www.ncbi.nlm.nih.gov/pmc/articles/PMC154479/pdf/cdg188.pdf

43. Spina CA, Anderson J, Archin NM, Bosque A, Chan J, Famiglietti M, et al. An In-Depth Comparison of Latent HIV-1 Reactivation in Multiple Cell Model Systems and Resting CD4+ T Cells from Aviremic Patients. Emerman M, editor. PLoS Pathog [Internet]. 2013 Dec 26;9(12):e1003834. Available from: http://dx.plos.org/10.1371/journal.ppat.1003834

44. Spivak AM, Planelles V. Novel Latency Reversal Agents for HIV-1 Cure. Annu Rev Med [Internet]. 2018 Jan 29 [cited 2018 Aug 15];69(1):421–36. Available from: https://www.ncbi.nlm.nih.gov/pmc/articles/PMC5892446/

45. Hoggatt J, Hoggatt AF, Tate TA, Fortman J, Pelus LM. Bleeding the laboratory mouse: Not all methods are equal. Exp Hematol [Internet]. 2016;44(2):132-137.e1. Available from: http://dx.doi.org/10.1016/j.exphem.2015.10.008

46. Slørdal L, Muench MO, Warren DJ, Moore MAS. Radioprotection by murine and human tumor-necrosis factor: Dose-dependent effects on hematopoiesis in the mouse. Eur J Haematol. 1989;43(5):428–34.

47. Namikawa R, Kaneshima H, Lieberman M, Weissman IL, McCune JM. Infection of the SCID-hu mouse by HIV-1. Science (80-). 1988;242(4886):1684–6.

48. Symons J, Cameron PU, Lewin SR. HIV integration sites and implications for maintenance of the reservoir. Curr Opin HIV AIDS [Internet]. 2018 Mar;13(2):152–9. Available from: http://insights.ovid.com/crossref?an=01222929-201803000-00009

49. Anderson EM, Maldarelli F. The role of integration and clonal expansion in HIV infection: Live long and prosper 11 Medical and Health Sciences 1108 Medical Microbiology Ben Berkhout, Alexander Pasternak. Retrovirology [Internet]. 2018;15(1):1–22. Available from: https://doi.org/10.1186/s12977-018-0448-8

50. Maldarelli F, Wu X, Su L, Simonetti FR, Shao W, Hill S, et al. Specific HIV integration sites are linked to clonal expansion and persistence of infected cells. Science (80-) [Internet]. 2014 Jul 11;345(6193):179–83. Available from: https://www.sciencemag.org/lookup/doi/10.1126/science.1254194

51. Abdel-Mohsen M, Chavez L, Tandon R, Chew GM, Deng X, Danesh A, et al. Human Galectin-

9 Is a Potent Mediator of HIV Transcription and Reactivation. PLoS Pathog [Internet]. 2016;12(6):1–28. Available from: http://dx.doi.org/10.1371/journal.ppat.1005677

52. Jiang G, Mendes EA, Kaiser P, Wong DP, Tang Y, Cai I, et al. Synergistic Reactivation of Latent HIV Expression by Ingenol-3-Angelate, PEP005, Targeted NF-kB Signaling in Combination with JQ1 Induced p-TEFb Activation. PLoS Pathog. 2015;11(7):1–27.

53. Darcis G, Kula A, Bouchat S, Fujinaga K, Corazza F, Ait-Ammar A, et al. An In-Depth Comparison of Latency-Reversing Agent Combinations in Various In Vitro and Ex Vivo HIV-1 Latency Models Identified Bryostatin-1+JQ1 and Ingenol-B+JQ1 to Potently Reactivate Viral Gene Expression. PLoS Pathog. 2015;11(7):1–36.

54. Reuse S, Calao M, Kabeya K, Guiguen A, Gatot JS, Quivy V, et al. Synergistic activation of HIV-1 expression by deacetylase inhibitors and prostratin: Implications for treatment of latent infection. PLoS One. 2009;4(6).

55. Brogdon J, Ziani W, Wang X, Veazey RS, Xu H. In vitro effects of the small-molecule protein kinase C agonists on HIV latency reactivation. Sci Rep [Internet]. 2016;6(November):1–8. Available from: http://dx.doi.org/10.1038/srep39032

56. Chen D, Wang H, Aweya JJ, Chen Y, Chen M, Wu X, et al. HMBA Enhances Prostratin-Induced Activation of Latent HIV-1 via Suppressing the Expression of Negative Feedback Regulator A20/TNFAIP3 in NF- B Signaling. Biomed Res Int. 2016;2016.

57. Rochat MA, Schlaepfer E, Speck RF. Promising Role of Toll-Like Receptor 8 Agonist in Concert with Prostratin for Activation of Silent HIV. J Virol. 2017;91(4):1–21.

58. Klase Z, Yedavalli VSRK, Houzet L, Perkins M, Maldarelli F, Brenchley J, et al. Activation of HIV-1 from Latent Infection via Synergy of RUNX1 Inhibitor Ro5-3335 and SAHA. PLoS Pathog. 2014;10(3).

59. Bouchat S, Delacourt N, Kula A, Darcis G, Van Driessche B, Corazza F, et al. Sequential treatment with 5-aza-2'-deoxycytidine and deacetylase inhibitors reactivates HIV -1 . EMBO Mol Med. 2016;8(2):117–38.

60. Kutsch O, Wolschendorf F, Planelles V. Facts and Fiction: Cellular Models for High Throughput Screening for HIV-1 Reactivating Drugs. Curr HIV Res [Internet]. 2011 Dec 1;9(8):568–78. Available from: http://www.eurekaselect.com/openurl/content.php?genre=article&issn=1570-162X&volume=9&issue=8&spage=568

61. Bradley T, Ferrari G, Haynes BF, Margolis DM, Browne EP. Single-Cell Analysis of Quiescent HIV Infection Reveals Host Transcriptional Profiles that Regulate Proviral Latency. Cell Rep [Internet]. 2018 Oct;25(1):107-117.e3. Available from: https://linkinghub.elsevier.com/retrieve/pii/S2211124718314505

62. Telwatte S, Morón-López S, Aran D, Kim P, Hsieh C, Joshi S, et al. Heterogeneity in HIV and cellular transcription profiles in cell line models of latent and productive infection: implications for HIV latency. Retrovirology [Internet]. 2019;16(1):32. Available from: https://doi.org/10.1186/s12977-019-0494-x

63. Dahl V, Gisslen M, Hagberg L, Peterson J, Shao W, Spudich S, et al. An example of genetically distinct HIV type 1 variants in cerebrospinal fluid and plasma during

suppressive therapy. J Infect Dis. 2014;209(10):1618–22.

64. T. Blackard J. HIV Compartmentalization: A Review on a Clinically Important Phenomenon. Curr HIV Res. 2012;10(2):133–42.

65. Telwatte S, Lee S, Somsouk M, Hatano H, Baker C, Kaiser P, et al. Gut and blood differ in constitutive blocks to HIV transcription, suggesting tissue-specific differences in the mechanisms that govern HIV latency. PLoS Pathog. 2018;14(11):1–28.

66. Thompson KA, Cherry CL, Bell JE, McLean CA. Brain cell reservoirs of latent virus in presymptomatic HIV-infected individuals. Am J Pathol [Internet]. 2011;179(4):1623–9. Available from: http://dx.doi.org/10.1016/j.ajpath.2011.06.039

67. Castellano P, Prevedel L, Valdebenito S, Eugenin EA. HIV infection and latency induce a unique metabolic signature in human macrophages. Sci Rep [Internet]. 2019;9(1):1–14. Available from: http://dx.doi.org/10.1038/s41598-019-39898-5

68. Wong ME, Jaworowski A, Hearps AC. The HIV Reservoir in Monocytes and Macrophages. Front Immunol [Internet]. 2019 Jun 26;10(JUN). Available from: https://www.frontiersin.org/article/10.3389/fimmu.2019.01435/full

69. Abreu CM, Veenhuis RT, Avalos CR, Graham S, Parrilla DR, Ferreira EA, Queen SE, Shirk EN, Bullock BT, Li M, Metcalf Pate KA, Beck SE, Mangus LM, Mankowski JL, Mac Gabhann F, O'Connor SL, Gama L CJ. Myeloid and CD4 T Cells Comprise the Latent Reservoir in Antiretroviral Therapy-Suppressed SIVmac251-Infected Macaques. 2019;10(4):1–19.

70. Gray LR, On H, Roberts E, Lu HK, Moso MA, Raison JA, et al. Toxicity and in vitro activity of

HIV-1 latency-reversing agents in primary CNS cells. J Neurovirol [Internet]. 2016 Aug 4;22(4):455–63. Available from: http://link.springer.com/10.1007/s13365-015-0413-4

71. Hellmuth J, Valcour V, Spudich S. CNS reservoirs for HIV: implications for eradication. J virus Erad [Internet]. 2015;1(2):67–71. Available from: http://www.ncbi.nlm.nih.gov/pubmed/26430703%0Ahttp://www.pubmedcentral.nih.gov/articlerender.fcgi?artid=PMC4586130

72. Folks TM, Justement J, Kinter A, Dinarello CA, Fauci AS, Folks TM, et al. Cytokine-Induced Expression of HIV-1 in a Chronically Infected Promonocyte Cell Line. Science (80-) [Internet]. 1987;238(4828):800–2. Available from: https://www.jstor.org/stable/1700363

73. Joseph SB, Arrildt KT, Sturdevant CB, Swanstrom R. HIV-1 target cells in the CNS. J Neurovirol [Internet]. 2015 Jun 19;21(3):276–89. Available from: http://link.springer.com/10.1007/s13365-014-0287-x

74. Barat C, Proust A, Deshiere A, Leboeuf M, Drouin J, Tremblay MJ. Astrocytes sustain long-term productive HIV-1 infection without establishment of reactivable viral latency. Glia [Internet]. 2018 Jul [cited 2018 Aug 15];66(7):1363–81. Available from: https://onlinelibrary.wiley.com/doi/abs/10.1002/glia.23310

75. Edén A, Fuchs D, Hagberg L, Nilsson S, Spudich S, Svennerholm B, et al. HIV-1 Viral Escape in Cerebrospinal Fluid of Subjects on Suppressive Antiretroviral Treatment. J Infect Dis. 2010;202(12):1819–25.

76. Churchill M, Nath A. Where does HIV hide? A focus on the central nervous system. Curr

Opin HIV AIDS [Internet]. 2013 May;8(3):165–9. Available from: http://content.wkhealth.com/linkback/openurl?sid=WKPTLP:landingpage&an=01222929-201305000-00003

77. Nath A, Clements JE. Eradication of HIV from the brain: Reasons for pause. Aids. 2011;25(5):577–80.

78. Tyor WR, Power C, Gendelman HE, Markham RB. A model of human immunodeficiency virus encephalitis in scid mice. Proc Natl Acad Sci U S A. 1993;90(18):8658–62.

79. Potula R, Poluektova L, Knipe B, Chrastil J, Heilman D, Dou H, et al. Inhibition of indoleamine 2 , 3-dioxygenase (IDO) enhances elimination of virus-infected macrophages in an animal model of HIV-1 encephalitis. 2005;106(7):2382–90.

80. Poluektova LY, Munn DH, Persidsky Y, Gendelman HE. Generation of Cytotoxic T Cells Against Virus-Infected Human Brain Macrophages in a Murine Model of HIV-1 Encephalitis. J Immunol. 2002;168(8):3941–9.

81. Poluektova L, Gorantla S, Faraci J, Birusingh K, Dou H, Gendelman HE. Neuroregulatory Events Follow Adaptive Immune-Mediated Elimination of HIV-1-Infected Macrophages: Studies in a Murine Model of Viral Encephalitis. J Immunol [Internet]. 2004 Jun 15;172(12):7610–7. Available from: http://www.jimmunol.org/lookup/doi/10.4049/jimmunol.172.12.7610

82. Persidsky Y, Limoges J, McComb R, Bock P, Baldwin T, Tyor W, et al. Human immunodeficiency virus encephalitis in SCID mice. Am J Pathol. 1996;149(3):1027–53.

83. Garcia-mesa Y, Jay TR, Checkley MA, Luttge B, Dobrowolski C, Valadkhan S, et al. Immortalization of primary microglia: a new platform to study HIV regulation in the central nervous system. J Neurovirol [Internet]. 2017 [cited 2018 Sep 5];23(1):47–66. Available from: https://www.ncbi.nlm.nih.gov/pmc/articles/PMC5329090/

84. Alvarez-Carbonell D, Garcia-Mesa Y, Milne S, Das B, Dobrowolski C, Rojas R, et al. Toll-like receptor 3 activation selectively reverses HIV latency in microglial cells. Retrovirology [Internet]. 2017;14(1):9. Available from: http://retrovirology.biomedcentral.com/articles/10.1186/s12977-017-0335-8

85. Yin C, Zhang T, Qu X, Zhang Y, Putatunda R, Xiao X, et al. In Vivo Excision of HIV-1 Provirus by saCas9 and Multiplex Single-Guide RNAs in Animal Models. Mol Ther [Internet]. 2017 May 3 [cited 2018 Aug 16];25(5):1168–86. Available from: http://www.sciencedirect.com/science/article/pii/S1525001617301107

86. Dash PK, Kaminski R, Bella R, Su H, Mathews S, Ahooyi TM, et al. Sequential LASER ART and CRISPR Treatments Eliminate HIV-1 in a Subset of Infected Humanized Mice. Nat Commun [Internet]. 2019;10(1):1–20. Available from: http://dx.doi.org/10.1038/s41467-019-10366-y

87. Tebas P, Stein D, Tang WW, Frank I, Wang SQ, Lee G, et al. Gene Editing of CCR5 in Autologous CD4 T Cells of Persons Infected with HIV. N Engl J Med [Internet]. 2014 Mar 6 [cited 2019 Nov 15];370(10):901–10. Available from: http://www.ncbi.nlm.nih.gov/pubmed/24597865

88. Jordan A, Defechereux P, Verdin E. The site of HIV-1 integration in the human genome

determines basal transcriptional activity and response to Tat transactivation. EMBO J. 2001;20(7):1726–38.

89. Beyer AI, Muench MO. Comparison of human hematopoietic reconstitution in different strains of immunodeficient mice. Stem Cells Dev. 2017;26(2):102–12.